Pressure-Induced Polymerization of Carbon Monoxide: Disproportionation and Synthesis of an Energetic Lactonic Polymer

W. J. Evans,* M. J. Lipp, C.-S. Yoo, H. Cynn, J. L. Herberg, and R. S. Maxwell

Lawrence Livermore National Laboratory, 7000 East Avenue, Livermore, California 94551

M. F. Nicol

University of Nevada Las Vegas, Las Vegas, Nevada 89154-4002

Received November 6, 2005. Revised Manuscript Received February 27, 2006

We have studied pressure-induced chemical reactions in carbon monoxide using both a diamond anvil cell and a modified large volume press. Our spectroscopic data reveal that carbon monoxide disproportionates into molecular CO_2 and a solid lactone-type polymer; photochemically above 3.2 GPa, thermochemically above 5 GPa at 300 K, or at 3 GPa and ~2000 K as achieved by laser heating. The solid product can be recovered at ambient conditions with a high degree of conversion, measured to be up to 95% of the original CO. Its fundamental chemical structure includes β-lactone and conjugated C═C, which can be considered a severely modified polymeric carbon suboxide with open ladders and smaller five-membered rings. The polymer is metastable at ambient conditions, spontaneously liberating CO_2 gases exothermically. We find that the recovered polymer has a high energy density, 1−8 kJ/g, and is very combustible. We estimate the density of recovered CO polymer to be at least 1.65 g/cm^3.

Introduction

Condensed carbon monoxide (CO) has received a great deal of attention for many reasons, including comparisons to iso-electronic nitrogen (N_2) with strong analogies at low pressures and marked differences at high pressures,[1,2] their similar behaviors under shock compression,[3,4] and in particular its pressure-induced transformations to nonmolecular phases.[5,6] At low pressures, CO and N_2 crystallize into the same disordered hexagonal solid (β-phase, $P6_3/mmc$) and then transform into ordered cubic structures (α-phase, $P2_13$ in CO and $Pa3$ in N_2) on further cooling. At ambient temperatures, CO and N_2 crystallize into the β-phase at around 2 GPa and then into an ordered cubic structure (δ-phase, $Pm3n$) near 4.0 GPa. The high-pressure behavior of the δ-phase, however, diverges greatly between CO and N_2. δ-CO is not stable above 5 GPa and transforms irreversibly to a colored, nonmolecular phase.[5] In contrast, molecular N_2 is stable over a wide range of pressures, undergoing a series of phase transitions from δ-N_2 to ϵ-N_2 at 20 GPa, to ζ-N_2 at 60 GPa, and finally to the nonmolecular, probably amorphous, η-phase above 160 GPa.[6−8] Recently, it has also been reported that laser-heated N_2 transforms to yet another nonmolecular *cubic gauche* (*cg*)-N phase ($I2_13$) above 110 GPa and 2000 K.[9] It is not known, however, whether there is any relationship between the nonmolecular η and *cg*-N phases, nor are there any data regarding their predicted novel properties such as the high energy content.[10] Indeed, pressure-induced polymerization has been observed in a number of molecular systems, such as hydrogen cyanide[11] and acetylene,[12−16] with a strong potential of novel technologically important properties.

The subtle difference in chemical bonding between CO and N_2 leads to a dramatic divergence in their behaviors at high pressures, which provides fundamental and systematic data for condensed matter theory and solid-state chemistry under extreme conditions. Despite such a pivotal role, substantially less attention has been devoted to understanding the pressure-induced physical and chemical changes of CO.

Katz et al.[5] were the first to report the pressure-polymerized product of CO (which we shall refer to as p-CO) in a diamond anvil cell (DAC). Shortly after the initial discovery,

(1) Cromer, D. T.; Schiferl, D.; Lesar, R.; Mills, R. L. *Acta Crystallogr., Sect. C* **1983**, *39* (Sep), 1146−1150.
(2) Gregoryanz, E.; Goncharov, A. F.; Hemley, R. J.; Mao, H. K.; Somayazulu, M.; Shen, G. Y. *Phys. Rev. B* **2002**, *66* (22), 224108.
(3) Nellis, W. J.; Holmes, N. C.; Mitchell, A. C.; Vanthiel, M. *Phys. Rev. Lett.* **1984**, *53* (17), 1661−1664.
(4) Nellis, W. J.; Ree, F. H.; Vanthiel, M.; Mitchell, A. C. *J. Chem. Phys.* **1981**, *75* (6), 3055−3063.
(5) Katz, A. I.; Schiferl, D.; Mills, R. L. *J. Phys. Chem.* **1984**, *88* (15), 3176−3179.
(6) Eremets, M. L.; Hemley, R. J.; Mao, H.; Gregoryanz, E. *Nature* **2001**, *411* (6834), 170−174.
(7) Goncharov, A. F.; Gregoryanz, E.; Mao, H. K.; Liu, Z. X.; Hemley, R. J. *Phys. Rev. Lett.* **2000**, *85* (6), 1262−1265.
(8) Tassini, L.; Gorelli, F.; Ulivi, L. *J. Chem. Phys.* **2005**, *122* (7), 074701.
(9) Eremets, M. I.; Gavriliuk, A. G.; Trojan, I. A.; Dzivenko, D. A.; Boehler, R. *Nat. Mater.* **2004**, *3* (8), 558−563.
(10) Mailhiot, C.; Yang, L. H.; McMahan, A. K. *Phys. Rev. B* **1992**, *46* (22), 14419−14435.
(11) Mozhaev, P. S.; Kichigina, G. A.; Kiryukhin, D. P.; Barkalov, I. M. *High Energy Chem.* **1995**, *29* (1), 15−18.
(12) Aoki, K.; Kakudate, Y.; Yoshida, M.; Usuba, S.; Tanaka, K.; Fujiwara, S. *Synth. Met.* **1989**, *28* (3), D91−D98.
(13) Aoki, K.; Usuba, S.; Yoshida, M.; Kakudate, Y.; Tanaka, K.; Fujiwara, S. *J. Chem. Phys.* **1988**, *89* (1), 529−534.
(14) Lesar, R. *J. Chem. Phys.* **1987**, *86* (3), 1485−1490.
(15) Sakashita, M.; Yamawaki, H.; Aoki, K. *J. Phys. Chem.* **1996**, *100* (23), 9943−9947.
(16) Trout, C. C.; Badding, J. V. *J. Phys. Chem. A* **2000**, *104* (34), 8142−8145.

10.1021/cm0524446 CCC: $33.50
Published on Web 04/22/2006

they found that the recovered product was highly photosensitive, very sensitive to atmospheric moisture,[17] and continuously changed its color and texture, hampering further characterization.[5] They were unable to observe features in the Raman spectra of the product and speculated, on the basis of some similarities of the infrared spectra with those of polymerized carbon suboxide (poly-(C_3O_2)), specifically a sharp absorption edge at 3700 cm^{-1} and a maximum in transmission at 2200 cm^{-1}, that CO stoichiometrically disproportionates and polymerizes into poly-(C_3O_2), leaving behind some residual oxygen. Mills et al. observed that CO loses its X-ray diffraction peaks as the chemical reaction occurs at 5 GPa at room temperature.[18] They also found that the pressure threshold of the chemical instability and associated polymerization increased to ~12 GPa at 15 K. Lipp et al. were the first to actually show Raman, Fourier transform infrared (FT-IR), and absorption spectra of a sample that was converted by laser irradiation in the visible.[19] On the basis of their observations they concluded that the synthesized material was not a mixture of polymerized carbon suboxide and oxalic anhydride as suggested previously[20] but was composed of graphitic-like carbon, carbon dioxide, and a polymerized network containing vinyl ester-like groups such as −(C═O)−O−(C−)═C<. They suggested that the photochemical product was different from the one synthesized by compression alone and speculated that the solid CO disproportionated in this fashion: $6CO \rightarrow 2CO_2 + C + (C_3O_2)$ with the last entity representing the aforementioned vinyl ester-like group.

Ab initio molecular dynamics calculations indicated that the transformation might evolve in two steps on a picosecond time scale.[21] The polymerization was suggested to proceed without CO bond breaking when the individual molecules approached each other to closer than ~2.1 Å, and in contrast to the experiments, no formation of CO_2 molecules was observed. In the calculations, CO remained a molecular crystal at 200 K and 9.8 GPa, that is, well above the experimentally observed chemical instability. At 15 GPa the computer modeling predicted that the crystal initially changed to chemical bonding to form (0.25 ps) a simple polycarbonyl polymer, followed by more extended carbonyl polymers such as fivefold lactonic rings containing four carbon atoms (two carbonyl groups) and one ester bridge as well as linear segments that were partially interconnected. While these calculations seem to capture some detailed features of the CO pressure-induced reaction products, experimental challenges including the high reactivity, metastability, and minute amount of samples synthesized in DACs have hampered further chemical analyses and thus validation of the theoretical results.

The present study was undertaken to address the pressure-induced chemical reaction of carbon monoxide, that is, to characterize the pressure-synthesized products and to improve our understanding of the chemical reactions. Because of the experimental challenges mentioned above, no single experimental technique provides a complete characterization. Therefore, in this study we used several approaches and techniques including (i) in situ investigation of CO reaction in DAC, (ii) synthesis of the reaction products at the macroscopic scale of large volume presses, and (iii) characterizing chemical structures of the products by vibrational Raman and FT-IR spectroscopy, mass spectroscopy, magic angle spinning (MAS) solid-state ^{13}C NMR, solution-state ^{13}C NMR, and thermal analysis (differential scanning calorimetry, DSC). Details of some aspects of this work, such as the large volume synthesis of p-CO and its energetic properties, were recently published elsewhere.[22] In this paper, we review and expand on previous results, presenting new data to construct a more complete understanding of the properties of CO and its transformations at high pressures.

Experiment

The method for filling the sample chamber of a pressure cell with a highly toxic liquefied gas such as carbon monoxide involves construction of a leak-tight shield around the anvils enclosing the containment gasket. Careful consideration must to be given to several factors: (i) ease of operation; (ii) utilization of nonreactive materials; (iii) good thermal conductivity for cryogenic cooling; (iv) good gasket and loading system performance at the low temperatures necessary for loading liquid CO; (v) thermal isolation of the sample load chamber from ambient conditions; (vi) small dead volume to reduce stored energy and quantity of CO needed for loading; and (vii) for large volume presses, protection from shrapnel in case of failure of an anvil or gasket. In this study, we used a stainless steel metal bellows for the DAC and a brass or aluminum ring as the shield for the large volume press. A detailed discussion of this large volume press system is presented elsewhere.[23]

High purity CO (99.99+% from Matheson) was loaded into the sample chamber of a DAC. We used a Livermore-designed DAC of the LLL-type, a modified version of a Mao-Bell cell without a lever clamp, with 0.5 mm flat diamond anvils and a rhenium gasket. A small stainless steel metal bellows (~5 mm in diameter) was mounted around the diamond anvils and gasket to provide a vacuum-tight sample environment. To load liquid CO samples, the LLL cell was immersed into liquid N_2, the metal bellows enclosed sample area was evacuated to less than 50 mTorr, and CO gas was introduced at a pressure of about 2−3 atm through a small capillary tube. A sudden drop in the pressure in the CO supply line was taken to indicate condensation of the CO. After several minutes the diamond anvils were advanced to capture the liquid CO in the gasket hole. The excess amount of CO gas was diluted with a large amount of N_2 gas and released through a fume hood. All sample loading was performed inside a fume hood, and several CO warning detectors continuously monitored the air for any accidental release.

Despite the relatively modest synthesis conditions, the properties of p-CO remain largely unknown, owing to the microscopic amount of sample generated in the DAC experiments. To remedy this situation, we synthesized milligram quantities of p-CO at high pressures using a large volume press system, specifically, a modified

(17) Mills, R. Private communication (to C.-S. Yoo and M. Nicol).
(18) Mills, R. L.; Olinger, B.; Cromer, D. T. *J. Chem. Phys.* **1986**, *84* (5), 2837−2845.
(19) Lipp, M.; Evans, W. J.; Garcia-Baonza, V.; Lorenzana, H. E. *J. Low Temp. Phys.* **1998**, *111* (3−4), 247−256.
(20) Mills, R. L.; Schiferl, D.; Katz, A. I.; Olinger, B. W. *J. Phys.* **1984**, *45* (NC8), 187−190.
(21) Bernard, S.; Chiarotti, G. L.; Scandolo, S.; Tosatti, E. *Phys. Rev. Lett.* **1998**, *81* (10), 2092−2095.
(22) Lipp, M. J.; Evans, W. J.; Baer, B. J.; Yoo, C. S. *Nat. Mater.* **2005**, *4* (3), 211−215.
(23) Lipp, M. J.; Evans, W. J.; Yoo, C. S. *Rev. Sci. Instrum.* **2005**, *76* (5), 053903.

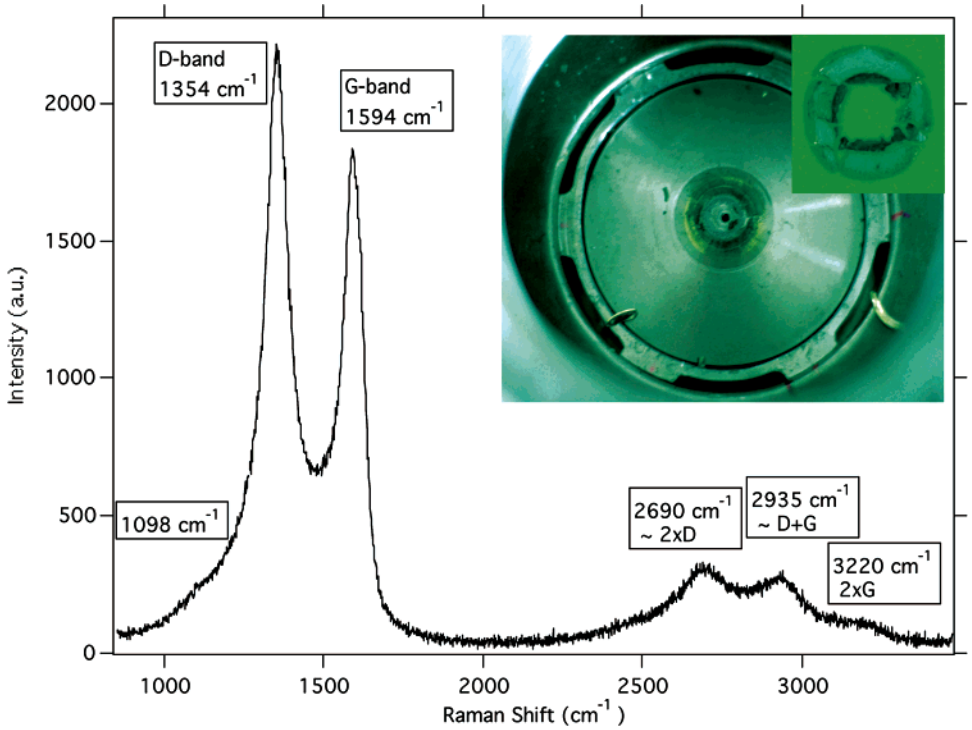

Figure 1. Raman spectrum of the black residue left at the center of a Bridgman anvil after a catastrophic failure during decompression. The inset shows the microphotographs of the Bridgman anvil and gasket remains recovered after the failure.

Paris-Edinburgh cell (mPEC).[23−25] High purity CO (99.99+%) was loaded into the mPEC sample chamber in the liquid phase at ∼10 bar and 80 K (liquid nitrogen). After capturing the CO sample, the system was warmed to room temperature; then the load on the sample was increased to the desired pressure for synthesis. For successful recovery we found it important to decompress the sample/gasket assembly *very* slowly. This requirement probably arises from the high mechanical energy built up on the sample chamber during loading and the high energy content of p-CO, both of which could result in a premature explosive failure.[26] Figure 1 shows the typical remains of a gasket after such a failure and the Raman spectrum of the residue (dark spot at the center of anvil). The Raman spectrum of the residue is typical of glassy carbon produced after an explosion of hydrocarbon materials exhibiting strong carbon D and G bands at around 1354 and 1594 cm^{-1} and their overtones/combination bands.

We have carried out angle-resolved X-ray diffraction experiments of the DAC-produced CO products at a third generation synchrotron source, optimized for DAC research (HPCAT, Advanced Photon Source, Argonne National Laboratory). The X-ray diffraction pattern of p-CO, however, consisted only of a very broad diffuse ring, analogous to that of amorphous or disordered phases. These results imply a lack of long-range order. The nature of the p-CO, such as metastability and amorphous structure, makes its characterization extremely challenging. A collection of analytical tools will be necessary to construct a coherent and thorough description of this material. Therefore, in the present study, we used several approaches, for example, vibrational spectroscopy for the in situ investigation in DAC and conventional analytical methods such as mass spectroscopy, NMR, and DSC.

A chamber was constructed to capture the gaseous products evolved from a p-CO sample synthesized in DAC. This chamber was easily coupled to a mass spectrometer (AEI MS 902) to analyze the emitted gases. The operating conditions were as follows: ion mass range 14−160, electron energies 16 and 70 eV, scan rates of 16 s/decade for low resolution and 34 s/decade for high resolution, and source temperatures of 24 °C for the gas samples and 200−300 °C for the solid products.

Solid products derived from isotopically enriched ^{13}CO were synthesized and analyzed using MAS ^{13}C NMR, which was performed on a Bruker Avance 500 MHz spectrometer with a magnetic field of 11.7 T. This gives a resonance frequency of 125.77 MHz for ^{13}C (spin = 1/2). The samples were packed in a Doty scientific insert, to center the sample, and placed in a 4 mm rotor. Spinning rates of 12 kHz were used. The free induction decay spectra were taken with a single excitation pulse. The ^{13}C NMR data were taken with a 90° pulse width of 8 μs. The ^{13}C NMR data were referenced to glycine at 32 ppm and 176.5 ppm.

We also measured infrared spectra of p-CO both in situ and as recovered using a commercial FT-IR spectrometer (Nicolet Magna 760). The spectrometer had been modified to incorporate a continuous and thorough nitrogen purge and a reflective condenser optical system (6:1) to accommodate the relatively small DAC sample size (∼300 micrometers in diameter). We used a liquid nitrogen cooled mercury cadmium telluride detector.

Raman scattering was excited using an argon ion laser, focused to a spot size of ∼15 μm with an incident power level of less than 20 mW at the sample. The Raman scattered light was collected at an angle of ∼30° with respect to the incident laser beam. The Raman signal was spatially filtered and analyzed using a holographic notch filter (Kaiser Optical Systems), a 0.3 m spectrograph (Instruments SA), and a liquid nitrogen cooled charge-coupled device detector (Princeton Instruments). Typical exposure times were 5 min.

Because the CO products might be a highly energetic material, we also performed DSC measurements. The DSC system was a commercial system (Perkin Elmer Pyris Diamond DSC). We used

(24) Besson, J. M.; Nelmes, R. J.; Hamel, G.; Loveday, J. S.; Weill, G.; Hull, S. *Physica B* **1992**, *180*, 907−910.
(25) Klotz, S.; Gauthier, M.; Besson, J. M.; Hamel, G.; Nelmes, R. J.; Loveday, J. S.; Wilson, R. M.; Marshall, W. G. *Appl. Phys. Lett.* **1995**, *67* (9), 1188−1190.
(26) Bundy, F. P. *Phys. Rep.* **1988**, *167* (3), 133−176.

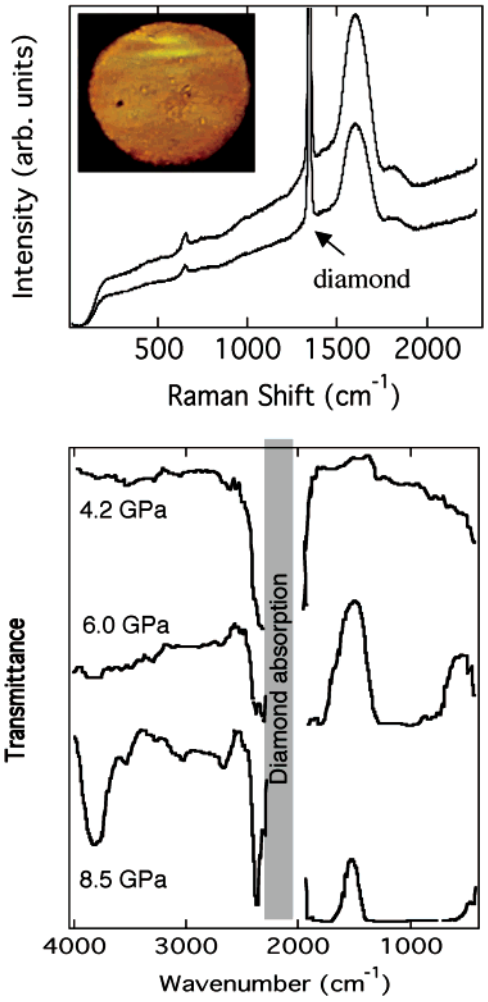

Figure 2. Microphotograph of "dark" reaction products of CO at 5.2 GPa and its associated Raman and FT-IR spectra. The Raman spectra were recorded from two different areas at the top of the sample (appearing as faint yellow stripes), and the FT-IR spectra were taken at different pressures.

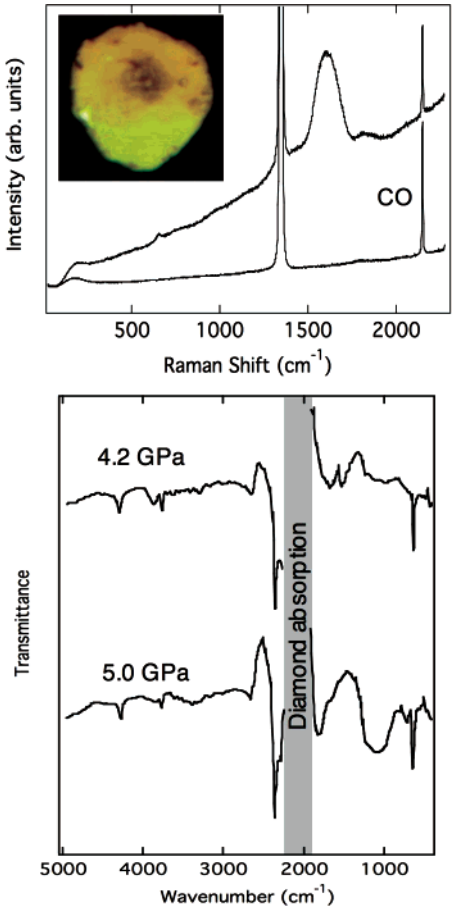

Figure 3. Microphotograph of "photo" reaction products of CO at 3.6 GPa and associated Raman and FT-IR spectra. The Raman spectra were obtained from a sample at 3.6 GPa by using weak 488 nm laser light: (bottom trace) at 1.5 mW for 300 s of exposure and (top trace) at 3 mW of power for 300 s to achieve conversion. The FT-IR spectra were obtained after sample exposure to weak 514 nm laser light at 4.2 GPa and after further compression to 5.0 GPa.

hermetically sealed gold pans that were carefully prepared to remove any contaminants. The DSC was operated to a maximum temperature of 600 °C with typical heating rates of 10 °C/min. The quantity of the sample was typically 2−5 mg.

Results

Carbon monoxide undergoes irreversible pressure-induced transformations to highly colored solid polymeric products. These transformations can be induced using pressure or alone or with added photochemical and thermochemical stimuli (Figures 2−4). When pressure alone is used, large milligram quantities of solid products (Figure 5) can be synthesized at 5−8 GPa at 300 K in a mPEC and then quenched to ambient conditions. At ambient conditions the products are metastable. IR, ^{13}C NMR, and mass spectroscopic analyses (Figure 6) indicate that these products are primarily composed of five- or six-membered lactone-type rings and conjugated C═C bonds with a high energy content rivaling or exceeding that of HMX (Figure 7). We discuss these results in further detail in the following sections.

A. Thermochemical "Dark" Reaction. At ambient temperature, the δ-phase of CO transforms to highly colored polymer-like products above ∼5.2 GPa. The transformed sample is a translucent yellow color, becoming increasingly red and dark as the thickness and, thus, optical density increase. Figure 2 shows such a sample while still at high pressure together with its vibrational Raman (collected at different locations) and FT-IR spectra (collected for the entire sample) over a range of pressures. The key features in the Raman spectra are at 650, 1600, and 1815 cm^{-1}, which we identify as the symmetric bending mode of CO_2, graphitic C═C stretching mode, and C═O stretching mode. Note that there is no indication of unreacted CO. The spectrum of unreacted CO would appear as a narrow band at ∼2140 cm^{-1} (see Figure 3, for example) which is totally absent in spectra of the transformed product.

The infrared spectra of the CO samples are not well-resolved because of the rather large sample thickness and strong absorptions bands of the products. As mentioned above, the transformed CO is highly absorptive, easily saturating absorption bands for samples thicker than a few micrometers. While no features are obvious at 4.2 GPa, broad peaks centered around 1000 and 1800 cm^{-1} are apparent from thick solid products at higher pressures, generated by C−O and C═O stretching modes, respectively. Further infrared absorptions at 3550 and 3800 cm^{-1}, particularly strong at 8.5 GPa, are believed to be overtones or combination bands involving carbonyl (C═O) stretches. If this is true, the absorption maxima of their fundamental bands should be at

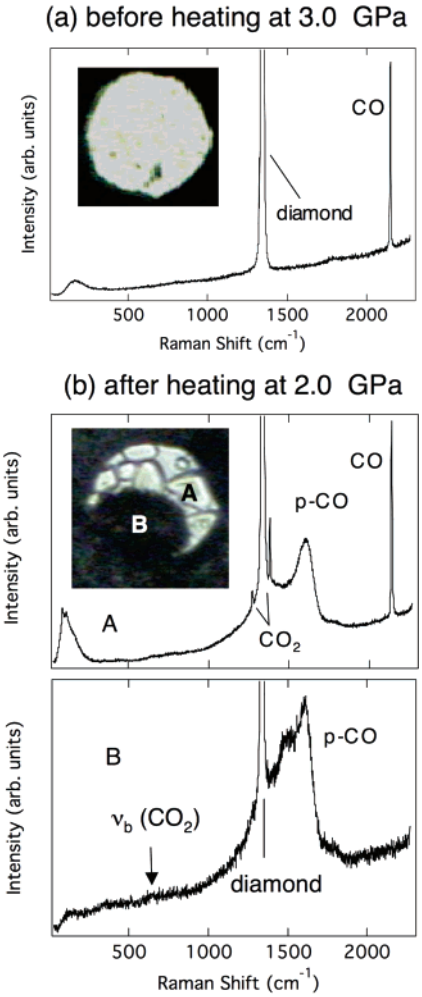

Figure 4. Microphotographs of unreacted CO before laser heating at 3.0 GPa and reaction products after the laser heating decreased the pressure to 2.0 GPa. The Raman spectra were taken from the transparent and opaque areas of the sample.

~1900 and 1775 cm^{-1}, far removed from the region ordinarily expected for carbonyl stretches, 1720−1760 cm^{-1}.[27] Nevertheless, it is important to note that the carbonyl vibrations for which two and/or three oxygen atoms are bonded directly to the carbonyl carbons occur precisely in the regions of 1750 and 1900 cm^{-1}.[27] Examples of this include carbonyls of anhydrides, five- or six-membered lactones, or cyclic carbonates.

As stated above the polymerized p-CO is metastable and can be pressure quenched and recovered to ambient conditions. However, not all of the transformed substance can be recovered to ambient conditions. During careful microscopic observation of a sample in a DAC we noted that a significant portion of the solid product converted to a liquid and evaporated during and immediately following a complete release of pressure. From the presence of CO_2 in the Raman spectra in Figure 2 (band at 2340 cm^{-1}), we attribute a decomposition mode of the metastable synthesized material to CO_2 molecules evolving from the solid product. In fact, our mass spectroscopic analysis of the gas products evolved from a sample synthesized in a DAC confirms the release of CO_2 and CO immediately after releasing the pressure and opening of the DAC. After complete relaxation of the pressure, we recovered a small piece of the highly colored polymeric solid p-CO in the gasket.

B. Photochemical Reaction. Intense visible laser light (e.g., 488 and 514 nm from Ar ion lasers) causes a similar chemical change in β-CO above 3.2 GPa, well below the 5.2 GPa threshold of the "dark" reaction. Figure 3 shows an image and the associated Raman and FT-IR spectra of a CO sample in a DAC after exposure to laser light in the range of 3−5 GPa. The Raman spectra were recorded from a sample at 3.6 GPa using 488 nm radiation at 1.5 mW for 300 s of exposure (bottom trace) and at 3 mW of power for 300 s (top trace) to achieve conversion. The Raman spectrum of the top trace again contains the three characteristic bands at 650, 1600, and 1815 cm^{-1}. The features are very similar to those of the "dark" products above 5.2 GPa, suggesting that the photochemical product is very similar to the dark (pressure only) product. The vibrational stretching mode ν_1 of unreacted CO is also apparent at 2140 cm^{-1}, particularly strong in the lighter yellow regions of the sample (inset in the top of Figure 3). The relative intensity of the unreacted

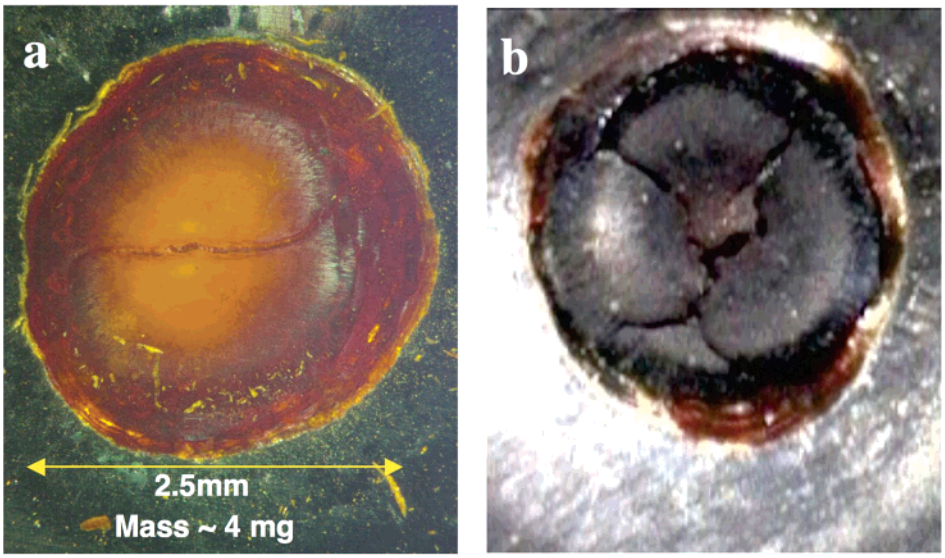

Figure 5. Microphotographs of milligram-quantity CO products, synthesized at ~6.7 and 7.0 GPa using a mPEC and quenched to ambient conditions, taken (a) under a microscope in reflection and (b) by a video camera.

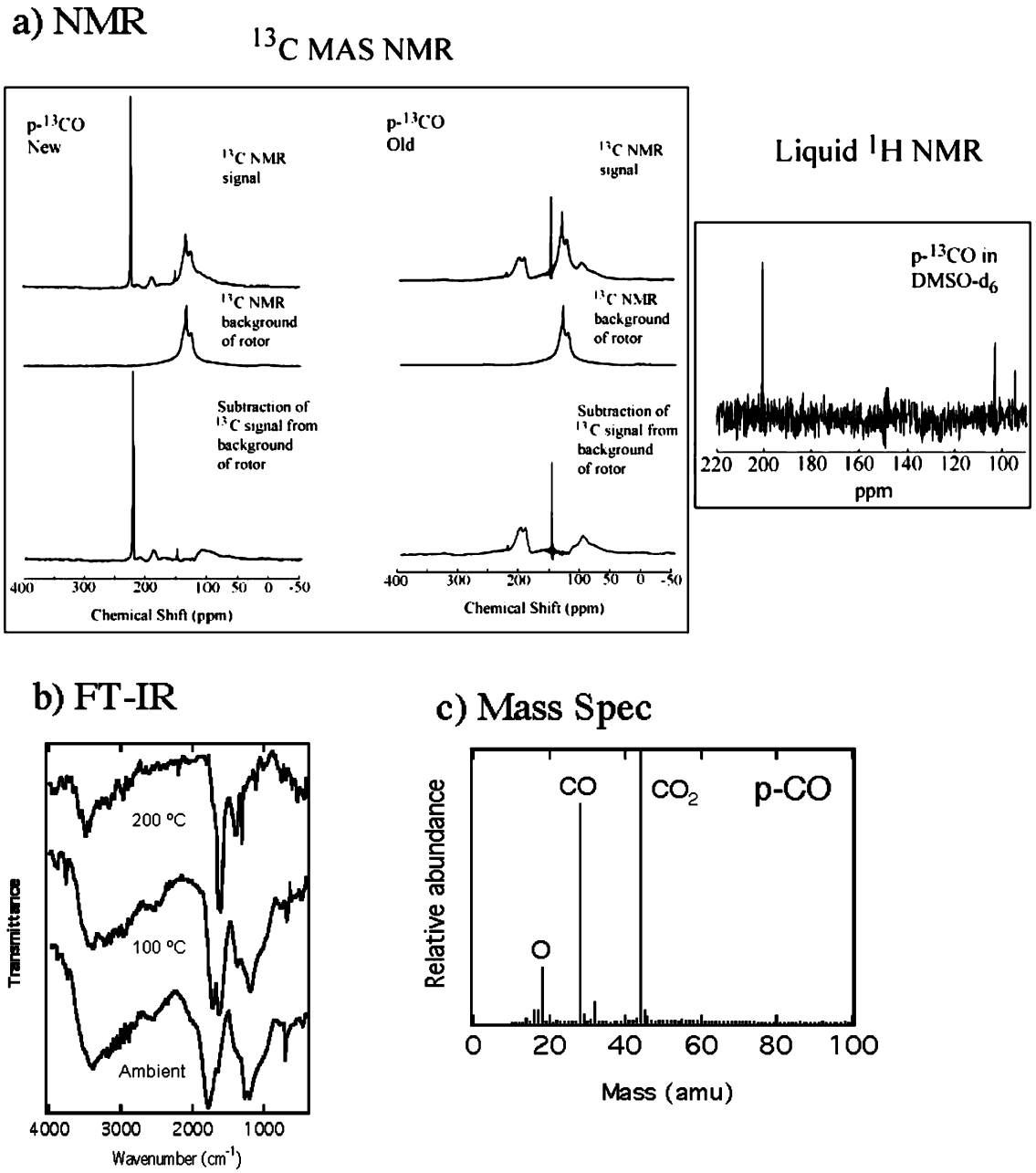

Figure 6. (a) MAS ^{13}C NMR spectra of p-^{13}CO recovered from 5.6 GPa (left), a 10 day old sample (middle), and p-CO in a DMSO-d_6 solution (right). (b) FT-IR spectra of recovered p-CO mulled in NaCl taken at different temperatures. (c) MS spectrum of recovered solid p-CO, showing main fragments of CO_2 and CO and their secondary fragment O.

CO peak is clearly less in the spectrum taken from the dark sample area, where the more intense laser was focused and thus the reaction had progressed further (see top of Figure 3).

FT-IR spectra taken at 4.2 GPa (see the lower panel in Figure 3) after weak laser exposure (20 mW at 514 nm for 5 min) exhibit two sharp peaks at 2375 and 675 cm^{-1}, slightly higher than the above-mentioned 3.2 GPa where the 488 nm laser exposure initiates the reaction. We identify these features as the stretching and bending modes of CO_2,[28] noting that they are not present without the exposure to the laser light at pressures below 5.0 GPa. At 5.0 GPa, a relatively opaque dark brown solid is produced at the location where the laser is focused, and strong broad features centered near 1150 and 1900 cm^{-1} appear in the infrared spectrum. These features are again similar to those of the dark (pressure only) reaction products. Untransformed carbon monoxide should have an infrared-active fundamental asymmetric stretching mode, ν_a, at around 2150 cm^{-1}, which is obscured by the strong diamond absorption.

The photo-assisted transformation products are also metastable, although there is some variation in stability with some products decomposing faster than others, again presumably by evolving CO_2, when quenched to ambient conditions. There are no apparent differences in either visual appearance or vibrational spectra between the dark pressure-only and the photo-assisted reaction products. The in situ spectroscopic Raman and FT-IR studies demonstrate that the photo-assisted

(27) Silverstein, R.; Webster, F. *Spectrometric Identification of Organic Compounds*, 6th ed.; John Wiley & Sons: New York, 1997.
(28) Hanson, R. C.; Jones, L. H. *J. Chem. Phys.* **1981**, *75* (3), 1102−1112.

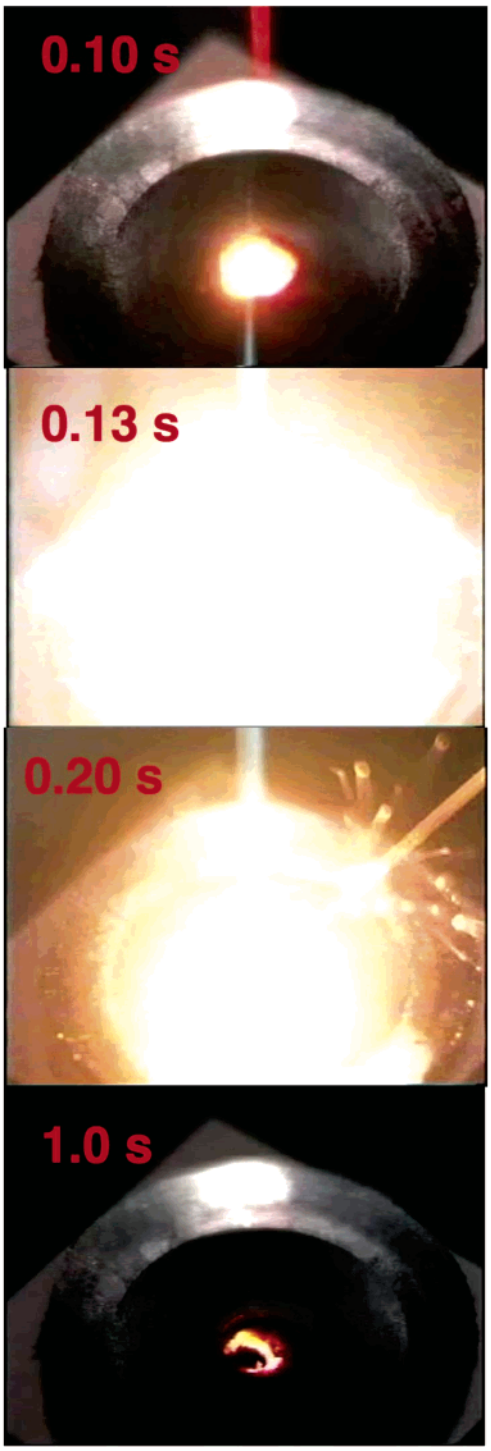

Figure 7. Video images of a p-CO sample initiated by a continuous wave YAG laser ($\lambda = 1064$ nm) with the elapsed time marked (in seconds) after the start of the exposure to the laser. The He−Ne laser (visible at the top frame) was used for alignment. The explosive energy release produces a plume of CO_2 gas that scatters the light from both He−Ne and YAG lasers leaving vertical streaks (red initially, but most of the time white). Note that the rate of energy release is highest at around 100−300 ms after the ignition (the second frame), during which period solid particles are violently ejected from the sample. The process continues for the next 0.5 s, after which only a small piece of black glassy carbon remains in the gasket (not shown).

reaction produces a type of polymeric CO very similar to the one produced under dark pressure only synthesis conditions. Both sets of conditions yield a product that evolves molecular CO_2, with the exception that the photo-assisted product appears to contain more CO_2 at an equivalent pressure. Our work also indicates that the amount of CO_2 produced increases with synthesis pressure. A plausible explanation is that the photo-assisted process and higher pressures may overdrive the transformation beyond the solid poly-CO product resulting in production of excess CO_2. Furthermore, the photo-assisted process requires uniform exposure of the sample to the laser stimulus, which if incomplete would lead to a sample that is only partially converted with more dangling bonds and thus inherently more unstable. Although the photochemical reaction is localized to places exposed to laser light, no obvious differences between the photo-assisted and dark products were found during further compression up to 40 GPa.

C. Thermochemical Reactions of Laser-Heated CO. A chemical transformation to the polymerized CO solid phase also occurs from different phases of carbon monoxide; for example, ϵ-CO transforms to the polymerized products at 10.0 GPa at 20 K and laser-heated CO transforms at pressures as low as 3 GPa, as shown in Figure 4. In this laser-heating experiment, the β-phase of solid CO (instead of the δ-phase) was heated at 3.0 GPa using a YLF laser (1053 nm). CO does not have an absorption band at this wavelength and thus does not absorb the 1053 nm light directly. To address this problem tiny ruby particles (appearing as black dots in the image of the CO sample) were used as radiation couplers, absorbing the 1053 nm light and converting it to heat. After heating, a part of the sample in the vicinity of the ruby particles nearly instantaneously transformed to an opaque material (see Figure 5b, inset). Because this change occurs rapidly, we are unable to determine whether the reaction started from solid β-CO or the solid first melted and then proceeded to polymerize from supercritical fluid CO. The transient temperature was estimated from pyrometry to have an upper bound of ~2000 K. It is important to note that this reaction occurred at ~3.0 GPa, again substantially lower than the ~5.2 GPa threshold of the dark pressure only synthesis. After laser heating and reaction, we also observed a relatively large pressure drop, of ~1.0 GPa. Because the sample chamber is approximately isochoric, this result suggests that the reaction products are more dense than the starting material. From basic mass and volume measurements, densities of solid p-CO product recovered from mPEC large volume press experiments were evaluated to be 1.65 g/cm^3, which is indeed substantially higher than that of β-CO at 3 GPa, ~1.4 g/cm^3, and more than twice the density of liquid CO. These measurements do not account for the porosity in the sample; thus, this value is a lower bound on the density.[29] In addition to the formation of the opaque region, parts of the transparent region of the sample turned into a mixture of two materials, as is evident from the grain boundaries in the inset of Figure 4b.

Figure 4a displays an image and Raman spectra of unreacted CO (top panel), and Figure 4b shows the spectra of the transparent (lower panel) and opaque product (upper panel) after laser heating. The vibrational features of the opaque product are similar to those of the "dark" and "photo-

(29) It was observed that the sample does not appear to fill the gasket hole completely after recovery because of the different elastic properties of the sample and gasket material as well as the loss of CO_2 and CO as recovered.

Table 1. MAS ^{13}C NMR of Solid p-^{13}CO Products versus Age and in Comparison with Solution ^{13}C NMR Taken in DMSO-d_6[a]

solid—new		solid—old		in DMSO-d_6		
ppm	intensity—width	ppm	intensity—width	ppm	intensity—width	assignments
223	vs—sh	224	w—sh	202	4.7—sh	—O—(C*═O)— or >C*═O
189	w—br	203	s—br			—C—(C*═O)—C—
		194	s—br			
151	w—sh	151	vs—sh	149	w—sh	>C*═C<
109	w—sh	100	s—br	103	2.9—sh	—(C═O)—O—C═C*
85	w—br	80	s—br	94	1.4—sh	—C*—O—(C═O)

[a] vs = very strong, s = strong, w = weak, sh = sharp, br = broad.

assisted" products described above. The Raman spectrum of the transparent area consists of CO_2 crystals (bands near 1273 and 1383 cm^{-1}), fluid CO (band at 2141 cm^{-1}), and nearby solid p-CO products (bands at 1607 and 1801 cm^{-1}). While the presence of CO_2 is apparent from its characteristic Fermi resonance bands, note that the CO_2 bending mode ν_b at 650 cm^{-1} is nearly absent in the Raman spectrum of transparent products (primarily CO_2 and a small amount of unreacted CO). This contrasts with the relatively strong ν_b intensity of the dark and photo-assisted products in Figures 2 and 3, clearly indicating a perturbation of the local inversion symmetry in CO_2 molecules in the dark and photo-assisted products. There is some residual, albeit very weak, intensity in the CO_2 bending mode in the Raman spectrum of the opaque product (marked by an arrow) in Figure 4b, consistent with those of the dark and photo-assisted products in Figures 2 and 3.

D. Synthesis of Milligram Quantities of Solid CO Products. We performed over 30 successful syntheses of p-CO using the mPEC. Recovered p-CO products had a variety of appearances, ranging over translucent orange, orange-brown, red-brown, and gray-red to name a few. We propose that these variations are the result of differing sample thicknesses and precise details of the synthesis conditions. Figure 5 shows two images of solid p-CO recovered after synthesis at 6.7 GPa (Figure 5a) and 7.0 GPa (Figure 5b) in a mPEC. These images provide examples of the wide variation in the optical characteristics of the samples. We find that we can achieve a product yield, that is, conversion from molecular CO, of up to 95% with the mPEC. The yield does not appear to correlate with either the color of the sample or details of synthesis in any discernible way. This may be due to uncertainties in the applied pressure, which was calculated from the applied load. An in situ pressure monitoring technique would be a better diagnostic of the pressure than the post mortem evaluation technique we have used.[30] Improved accuracy in our pressure measurement might elucidate a correlation between pressure and the nature of the product and yield. The recovered p-CO solid product was hygroscopic and photosensitive; its color ranged from milky white to brownish-orange as recovered and gradually darkened with time and exposure to light. The degree of metastability and rate of decomposition varied, with recovered product persisting from hours to weeks. Regardless of the decomposition rate, the product would continuously evolve CO_2 until simply carbon remained. As discussed above, the recovered product has a density of at least 1.65 g/cm^3. Thus it appears possible to "lock" the high density of the molecular solid at the transformation pressure into the recovered p-CO product. The texture of p-CO became gooey when exposed to air for several days or when immersed in organic solvents, including methanol or acetone. The solid product can be dissolved in deuterated dimethylsulfonyl oxide (DMSO-d_6). Raman spectra of recovered p-CO could not be obtained using visible argon ion laser radiation, which damaged and degraded the material because of its extremely high photosensitivity.

E. Characterization of the Chemical Structure of p-CO. In situ determination of the structure of p-CO is especially challenging because of the lack of long-range order resulting from the random polymer network. Nevertheless, a milligram quantity of recovered p-CO permits the determination of the chemical structure using solid-state MAS ^{13}C NMR, FT-IR, and mass spectrometry (MS). These spectroscopic results (summarized in Figure 6 and Table 1) suggest that p-CO is built from lactone-like carbonyls and conjugated C═C bonds in chemical configurations that can easily liberate CO_2 and convert to oxygen deficient graphitic C═C layers. The liberation of CO_2 is also consistent with our observations regarding the metastability and decomposition. The MAS ^{13}C NMR spectra of solid samples (Figure 6a) show two very sharp features at 223 and 151 ppm, characteristic of carbon atoms in ester- or lactone-like carbonyl groups and —O—(C═O)— and >C═C< double bonds, respectively.[27] After several days, the relative intensity of the 223 peak substantially decreases, while that of the 151 peak grows (see Figure 6b). Two broad features at ~189 and 109 ppm are identified as carbon atoms attached to the ester bridge of the —O—(C═O)— group and single-bonded carbon atoms coupled to an oxygen bridge or alternatively just singly bonded carbons. Both of these features gain intensity and develop sidebands over time scales of several hours to days. We identified similar sharp features at around 202 and 149 ppm when the product was dissolved into DMSO-d_6, as shown in the third panel of Figure 6a.

IR spectra were collected to study the effect of temperature and to gain insights into the stability and decomposition modes of the recovered p-CO. The infrared spectra of the recovered p-CO solid product, mulled with NaCl and heated to two different temperatures for 24 h, are presented in Figure 6b, with the energies of the peak positions summarized in Table 2. Mulling was necessary to reduce the concentration of the p-CO, which would otherwise have simply yielded spectra with saturated absorption bands. Several vibrational bands overlap, producing the broad feature centered at 1780 cm^{-1}. Two of them, at 1780 and 1800 cm^{-1}, are the carbonyl

(30) Lipp, M. J.; Evans, W. J.; Yoo, C. S. *High Pressure Res.* **2005**, *25* (3), 205—210.

Table 2. Vibrational Bands: Photo-Assisted, Thermally Treated, and Recovered

frequency (cm^{-1})						
8.7 GPa	ambient pressure					
25°C	25 °C	100 °C	200 °C	spectr. type	vibrational mode assignments	std ref value
3815				IR	2*[C—(C═O)—O]	
3533				IR	2*[C—(C═O)—O]	
2365				IR	CO_2 stretch	
1900	1800			IR	C—(C═O)—O in 5-lactone ring	1750−1800
1815				Raman	C—(C═O)—O	
	1780	1720		IR	C—(C═O)—O in 6-lactone ring	1720−1760
	1650	1630	1640	IR	C═C in unsaturated lactone	1660−1685
			1600			
1600				Raman	C═C	1600
	1400	1380	1400	IR	?	
			1360	IR	?	
	1200	1190		IR	—C—(C═O)—C— stretch	1150−1280
1180				IR	C—O—C in lactone	
	1000	1000		IR	C—O of unconjugated linear chain anhydride	
	710	690		IR	—C═C—	<720
677				IR	CO_2 bending	
650				Raman	CO_2 bending	

vibrations corresponding to the broad features centered in the in situ spectra of p-CO at 8.7 GPa in Figure 2. However, the energies are lower than expected when one interprets the peak at 3815 cm^{-1} as an overtone, whereas the band at 3533 cm^{-1} might well be one. Moreover, the large pressure dependence of the stretching mode as well as further chemical changes due to loss of CO_2 and CO should also be reflected in a shift of the carbonyl vibration to lower energies. During heating to 100 °C the high energy carbonyl vibration disappears first, while the energy of the other shifts down to 1720 cm^{-1}, and it disappears on further heating to 200 °C. The bands at 1275 and 1200 cm^{-1} and the shoulders at 1650 and 1400 cm^{-1} are consistent with the vibrations of C—(C═O)—O and O—C—C and C═C in cyclic systems.[27] Therefore, incorporating these observations into a unified interpretation, we propose that the structure of the solid product involves an unsaturated lactonic ring with five and/or six members at ambient temperature with the C═C bond adjacent to the —O— bridge. As the temperature increases, the absorption band of the lactone shifts to lower energy until it disappears, while the absorption strength of the C═C stretch is enhanced. This is related to the chemical changes that result from the liberation of CO_2 and CO molecular units, which are further reflected in color changes of the product during decomposition.

The MS spectrum of p-CO (Figure 6c) exhibits three main fragments: 44 amu for CO_2, 28 amu for CO, and 16 amu for O; O and CO are the secondary fragments of CO_2 and CO. Larger molecular fragments were not observed suggesting the p-CO is indeed unstable and prone to decompose into simple CO_2 and CO units under MS conditions. After the MS run we noted a black residue left on the source probe. This residue appeared to be graphitic carbon or simply carbon "soot". We found that similar gaseous products evaporated when the product was dissolved into DMSO-d_6.[31] We concede that the MS does not definitively identify the composition of p-CO and polymeric carbon suboxide (p-(C_3O_2)) also evolves CO_2 and CO without evidence of the parent molecule, C_3O_2.[32]

F. Characterization of Energy Content of p-CO. Recovery of macrosopic quantities of p-CO makes it possible to evaluate the material's energy content. A key question is whether this material is indeed a high energy density material similar to the theoretical predictions for nonmolecular *cg*-N.[10] There are some inherent difficulties in this measurement because p-CO is metastable, slowly releasing gaseous products such as CO_2 after recovery to ambient conditions. Nevertheless, our measurements represent a lower bound on the energy content. Though most conventional energetic materials are indefinitely stable, we emphasize that any energetic material is metastable by definition; that is, the system is kinetically impeded from releasing its energy and reconfiguring itself into a lower energy configuration. Because of this metastability of p-CO, our DSC results exhibit rather large sample-to-sample variations in the measured energy release of 1−8 kJ/g and location of the exotherm at 100−450 °C. We interpret these variations to be caused by the variations of the samples after recovery and/or the differences in the extent of their time-dependent degradation. However, these values are sufficient to establish that p-CO is indeed a high energy density material. Typical modern high explosives, such as TATB, RDX, and HMX, have thermal energy contents of 1−3 kJ/g.[33] An important qualifier for these measurements is that the DSC measures only thermal energy release. The total energy content, the sum of thermal energy and mechanical (pdV) work released, will be even larger given the CO_2 and CO gases produced by the decomposition.

The sequence of images obtained following laser initiation of the sample decomposition (Figure 7) further demonstrates that p-CO has a high energy content and behaves explosively when appropriately triggered. p-CO is rather sensitive and can readily be initiated even at a relatively weak laser power (<100 mW of Nd:YAG at $\lambda = 1064$ nm) and form a self-propagating front. To verify that the laser was not simply burning the sample, a subsequent exposure to the laser at

(31) Yoo, C.-S., Ph.D. Thesis, University of California—Los Angeles, Los Angeles, 1986.

(32) Yang, N. L.; Snow, A.; Haubenstock, H. *J. Polym. Sci., Part A: Polym. Chem.* **1978**, *16* (8), 1909−1927.

(33) Dobratz, B. M. *LLNL Explosive Handbook: Properties of Chemical Explosives and Explosive* Simulants; UCRL-52977, NTIS; Lawrence Livermore National Laboratory: Livermore, CA, 1985.

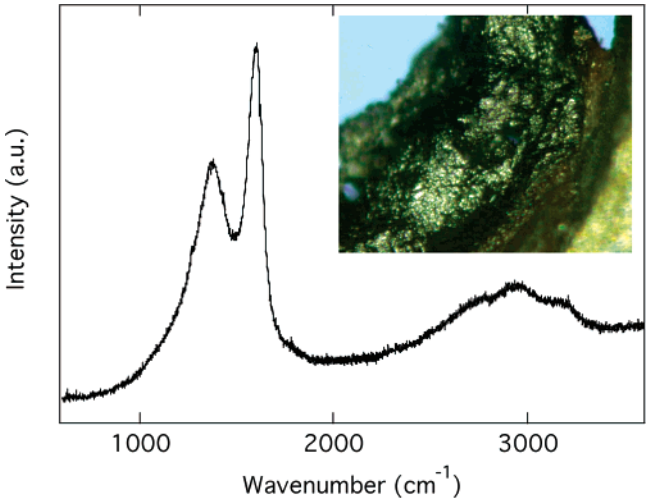

Figure 8. Raman spectrum of the residue after the explosive reaction of p-CO in Figure 7.

the same spot, now energetically spent, does not lead to another ignition. For comparison, at similar laser powers we found no effect on conventional energetic materials including PETN, NaN_3, and TATB. The ignition of these materials is a function of the absorption of the laser wavelength by the material, but it establishes that we are not simply observing combustion with the laser providing the thermal energy to ignite and burn the sample. On the basis of the intense incandescent emission from the initiated sample shown in Figure 7, the temperature was estimated to be well above 2500 K. The energetic decomposition of p-CO produces a large quantity of gaseous products. Using mass spectroscopy, we determined the product gases to be primarily CO_2. The final residue after the rapid decomposition (see inset of Figure 8) was characterized by Raman spectroscopy and determined to be glassy carbon[34] exhibiting the typical bands at 1350 and 1600 and their overtones at 2700−3200 cm^{-1}, very similar to the characteristic bands of the residue of a premature explosive failure during recovery unloading of a sample synthesized in the mPEC as shown in Figure 1. The strong presence of the characteristic D-band at 1350 cm^{-1} and its overtone at 2700 cm^{-1} indicates a substantial amount of sp^3 and sp disorder in sp^2 carbon species, similar to those produced after strong shock compression of hydrocarbons.[35]

Discussion

A. Pressure-Induced Disproportionation of CO. Our results clearly demonstrate that at room temperature CO undergoes an irreversible reaction that takes place photochemically at >3.2 GPa and thermochemically at >5.2 GPa. On the basis of the pressure−temperature data we have collected, we propose the chemical/phase diagram of CO in Figure 9. On the basis of the in situ IR and Raman spectroscopy of the converted CO in a DAC, we can confidently state that the reaction products include a polymeric solid, p-CO, and CO_2. It is important to note that when we refer to the polymeric solid, p-CO, it is derived from CO but is not stoichiometrically CO. Our spectroscopic work also demonstrates that the relative proportions of p-CO and CO_2 vary depending on the details of the reaction conditions. Nevertheless, the spectroscopic evidence that establishes the presence of these two components in the products of the pressure-induced transformation, regardless of conditions, demonstrates the disproportionation of CO at high pressures.

Several reaction pathways have been suggested in the past.[19,20] Pressure reduces the intermolecular distance, eventually destabilizing the CO molecule and initiating a reconfiguration of the bonds. A simple reaction would be a direct polymerization of CO forming a carbon backbone with oxygen groups bonded to the chain, −(C═O)−(C═O)−(C═O)−. However, the presence of CO_2 and the complexity of the NMR and IR spectra eliminate this as a possibility, and decomposition of this chain structure to p-CO is necessary to adequately account for the observed spectral

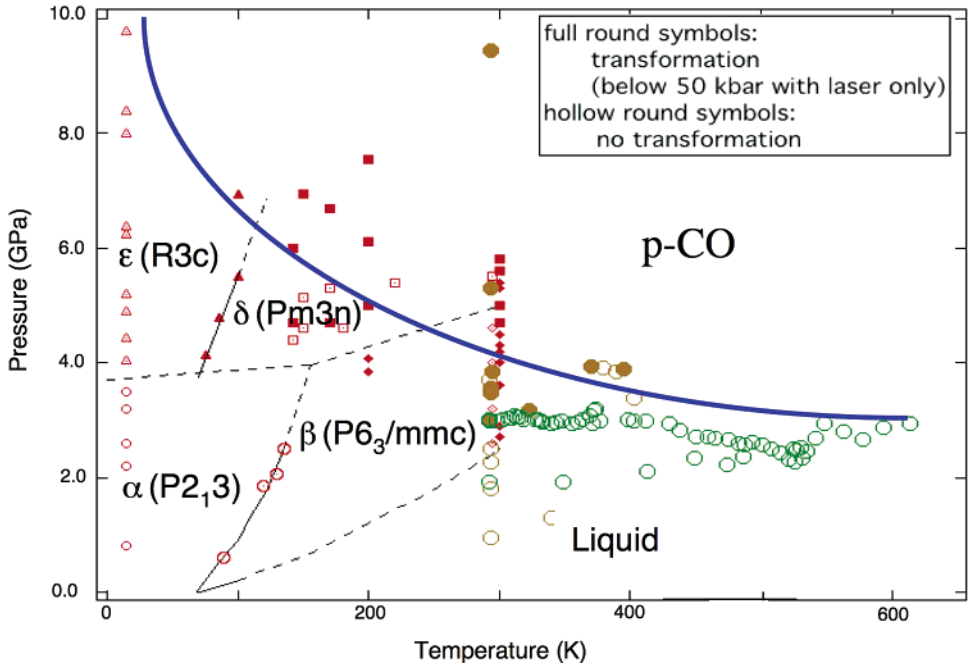

Figure 9. Chemical stability/phase diagram of carbon monoxide at high pressures. Filled and open symbols represent the reacted and unreacted CO samples, respectively.

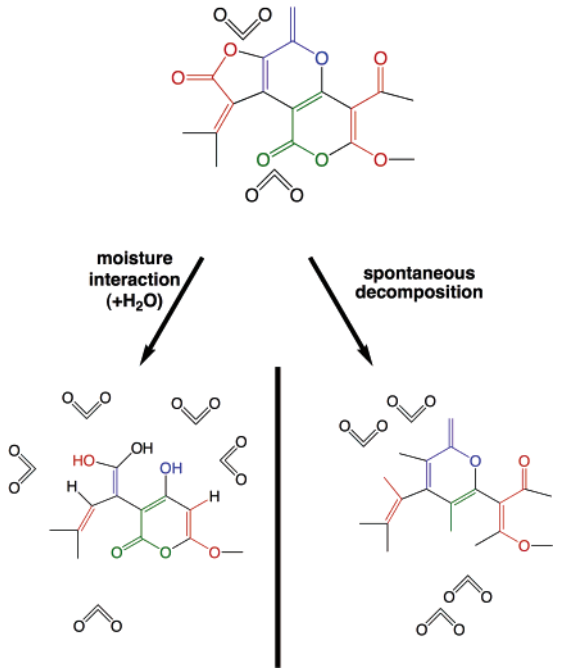

Figure 10. Proposed plausible structures of p-CO (showing associated CO_2) and possible liberation mechanisms of CO and CO_2 molecules resulting in its (chemical) metastability. The path on the left side depicts reaction with water, liberating CO_2. The path on the right side depicts spontaneous decomposition, liberating CO_2.

signatures. Thus, we arrive at a two-step process,

$$n(C{\equiv}O) \rightarrow (CO)_n \rightarrow \text{p-CO} + CO_2$$

Another possible reaction pathway, consistent with the data, could be disproportionation of the CO into carbon dioxide and carbon suboxide, followed by polymerization of the carbon suboxide forming p-CO and some residual carbon dioxide,

$$4CO \rightarrow CO_2 + C_3O_2$$

$$n(C_3O_2) \rightarrow (C_3O_2)_n \rightarrow \text{p-CO} + CO_2$$

A key feature distinguishing these two proposed reaction pathways is the disproportionation of CO, that is, prior to or following polymerization. If, as proposed by the first pathway, the disproportionation occurs following formation of an oxygen terminated carbon chain, a broad unconstrained range of daughter products can be achieved depending on the degree of disproportionation. Alternatively, the second reaction pathway has a stoichiometrically fixed amount of disproportionation. Measurement of the amount of CO_2 produced in the reaction might possibly be a tool to validate one of these proposals while eliminating the other. Unfortunately this approach to identifying the reaction pathway is difficult because the p-CO material is itself unstable, releasing CO_2 and complicating a measurement of the amount of CO_2 produced by the transformation.

By having recognized the above-mentioned difference, we can evaluate our measurements relative to a molecular structure of a quasi-random polycarbon suboxide $(C_3O_2)_n$, as illustrated in Figure 10. Then, our results supporting this model include (i) the strong presence of O—C═O and C═C—C species observed in both NMR and FT-IR, (ii) a chemical configuration that can easily liberate CO_2, (iii) a hygroscopic nature that can easily produce C—H and O—H bonds as observed in both NMR and FT-IR, and (iv) MS fragments of CO_2 and CO consistent with those of C_3O_2. Despite this support, there are important differences between p-CO and (C_3O_2):

(i) Hydrolysis of C_3O_2 typically yields CO_2 and CO with a 4:1 ratio at 250 °C, whereas our MS results show a substantially higher amount of CO evolving from p-CO.

(ii) Several strong IR bands are missing in p-CO, including the strong fundamental bands near 1365 and 1511 cm^{-1} that are characteristic of $(C_3O_2)_n$, whereas the broad feature at 3400 cm^{-1} observed in p-CO is missing in $(C_3O_2)_n$.

(iii) The estimated yield of p-CO, ~95%, is substantially higher than that expected from the formation of $(C_3O_2)_n$.[36]

(iv) Some of our experiments show only minute amounts of CO_2 following the polymerization, suggesting that much of the CO_2 is evolved in decomposition after the polymerization.

Therefore, we conclude that our measurements favor the latter model; that is, the pressure-induced polymerization followed by disproportionation. This model will certainly lead to more irregular structures than the $(C_3O_2)_n$ intermediate and produce a smaller amount of CO_2, as observed in the present study. Viewed from the perspective of polymeric carbon suboxide, p-CO can be thought of as an oxidized form of $(C_3O_2)_n$, that is, higher oxygen content.

In contrast to our experimental deductions, recent ab initio molecular dynamics calculations[21] suggest an entirely different transformation, neither disproportionation (CO_2 and $(C_3O_2)_n$) nor total polymerization. Despite differing reaction pathways, the theoretically predicted final structure of a partially interconnected polycarbonyl polymer with fivefold lactone-like units exhibits characteristics similar to those measured in the present study. One possible explanation of this discrepancy is that the theoretical simulation may be too tightly constrained to permit formation of multiple phases, or the time scale of the simulation is insufficient to capture the disproportionation process, if it proceeds relatively slowly.

B. Metastability. The solid p-CO product is metastable at ambient conditions. We remind the reader that the inversion symmetry of CO_2 is strongly perturbed in the dark pressure only and photo-assisted products at high pressures, for example, in Figures 2−4. A plausible interpretation of this is that CO_2 molecules are strongly associated with those solid products via chemisorption or physisorption. This conjecture is certainly consistent with the observed high yield of recovered p-CO which has an oxygen content similar to that of a highly oxidized state of $(C_3O_2)_n$. In this regard, p-CO can also be considered as a polymer, a severely perturbed analogue to $(C_3O_2)_n$, "supersaturated" with CO_2 at high pressures. One would expect this unique configuration to result in a material that is highly metastable upon pressure release or even a simple pressure−temperature change. The

(34) Knight, D. S.; White, W. B. *J. Mater. Res.* **1989**, *4* (2), 385−393.
(35) Yoo, C. S.; Nellis, W. J. *Science* **1991**, *254* (5037), 1489−1491.
(36) Smith, R. N.; Young, D. A.; Smith, E. N.; Carter, C. C. *Inorg. Chem.* **1963**, *2* (4), 829−838.

broad range of "oxidation" and CO_2 contents possible also provides an explanation for the wide range of variation in the color and properties of p-CO.

The recovered p-CO product is not indefinitely stable at ambient conditions and continuously decomposes by releasing CO_2 and CO molecules, while the color of the product darkens and gradually turns to black. Time sequences of vibrational spectra taken from the recovered p-CO (see Figure 6b or Table 2) showed the following changes: shifts of the carbonyl stretching to lower wavenumbers, an increase in the intensities of the carbon double bond stretching mode, and the disappearance of the carbonyl vibrational bands. Consistent with our observations, a degrading p-CO sample that contains fewer oxygen atoms near carbons will have carbonyl stretches that are less intense and centered at lower wavenumbers. Furthermore, in the spectrum at 200 °C in Figure 6b only the vibrational bands of the conjugated carbon double bond in the graphite-like molecules are present, with no evidence of any oxygen bonds. Loss of oxygen is also evident in the NMR spectrum, showing a remarkable enhancement of the C═C feature at 151 ppm with time (see Figure 6a). The color of conjugated polyene can be intensified by increasing the number of double bonds[37] as seen in the color changes in organic dyes and cyclic dienes, for example.[38] Therefore, it is likely that the metastability of recovered p-CO arises from relatively weak binding of CO_2 and carbonyl bonds which break liberating CO_2 and CO, increasing the number of conjugated carbon double bonds, and eventually forming a substance composed primarily of graphitic and glassy carbon phases.

C. Novel Energetic Content of p-CO. It has been suggested that the extended phases of low-*Z* molecular solids made of interconnecting strong covalent bonds are an entirely new class of materials that may exhibit novel properties including superhardness,[39] optical nonlinearity,[40] superconductivity,[41] and high energy density.[42] The present study clearly demonstrates for the first time that such novel materials can be synthesized at high pressures and recovered to ambient conditions, that is, the high energy content of p-CO, rivaling or exceeding that of HMX.

The energetic nature of p-CO is, in retrospect, not at all surprising. We note that the polymerization of carbon suboxide $(C_3O_2)_n$ has been observed to result in explosive energy release, as has already been reported previously.[43] Therefore, the high energy content of p-CO, similar in many respects to $(C_3O_2)_n$, should not be unexpected. We speculate that the energy release process would result in

$$\text{p-CO} \rightarrow CO_2 + \text{C(graphitic carbon)} + \text{energy}$$

the same decomposition process that makes p-CO metastable at ambient conditions. In this regard, considering that p-CO is a polymer saturated with CO_2 and a highly oxidized state of $(C_3O_2)_n$, one expects the energy content of p-CO to be substantially greater than that of $(C_3O_2)_n$. The quantitative measurement of the energy content, however, remains a challenge at the present time, again because of its metastability and environmental sensitivity. Therefore, control of the metastability appears to be the key issue in the further development of recovered p-CO as a new high explosive or energy source. The very moderate transition pressure, which is viable for industrial production, enhances the possibility of p-CO being developed for modern technological applications.

Acknowledgment. We thank Ken Visbeck for experimental help with the large volume press and HPCAT beamline scientist Dr. Maddury Somayazulu for technical assistance at beamline 16IDB. We also thank Milt Finger and Dr. William Holt for their enthusiastic support of this work. This work was performed under the auspices of the U.S. Department of Energy by University of California, Lawrence Livermore National Laboratory, under Contract No. W-7405-Eng-48 and at the University of Nevada Las Vegas under U.S. Department of Energy Cooperative Agreement FC08-01NV14049 and U.S. Army Research Office Contract No. W911NF-05-1-0266. Use of the HPCAT facility was supported by DOE-BES, DOE-NNSA (LLNL, UNLV, and CDAC), NSF, DOD-TACOM, and the W. M. Keck Foundation. Use of the Advanced Photon Source was supported by the U.S. Department of Energy, Office of Science, Office of Basic Energy Sciences, under Contract No. W-31-109-Eng-38.

CM0524446

(37) Herzberg, G. *Electronic spectra and electronic structure of polyatomic molecules*; Van Nostrand: New York, 1966; p 745.
(38) Mulliken, R. S. *J. Chem. Phys.* **1939**, *7* (5), 339−352.
(39) Yoo, C. S.; Cynn, H.; Gygi, F.; Galli, G.; Iota, V.; Nicol, M.; Carlson, S.; Hausermann, D.; Mailhiot, C. *Phys. Rev. Lett.* **1999**, *83* (26), 5527−5530.
(40) Iota, V.; Yoo, C. S.; Cynn, H. *Science* **1999**, *283* (5407), 1510−1513.
(41) Ashcroft, N. W. *Phys. Rev. Lett.* **2004**, *92* (18), 187002.
(42) Barbee, T. W.; McMahan, A. K.; Klepeis, J. E.; van Schilfgaarde, M. *Phys. Rev. B* **1997**, *56* (9), 5148−5155.
(43) Snow, A. W.; Haubenstock, H.; Yang, N. L. *Macromolecules* **1978**, *11* (1), 77−86.